Lab on a Chip

PAPER

View Article Online
View Journal | View Issue

Cite this: *Lab Chip*, 2015, **15**, 1294

Microfluidic single sperm entrapment and analysis†

B. de Wagenaar,*[a] J. T. W. Berendsen,[a] J. G. Bomer,[a] W. Olthuis,[a] A. van den Berg[a] and L. I. Segerink*[ab]

Received 4th December 2014,
Accepted 2nd January 2015

DOI: 10.1039/c4lc01425a

www.rsc.org/loc

Selection of healthy spermatozoa is of crucial importance for the success rates of assisted reproduction technologies (ART) such as *in vitro* fertilization and intra-cytoplasmic sperm injection. Although sperm selection for ART procedures is predominantly based on sperm motility, successful fertilization is not predicted by good motility alone. For example, sperm characteristics such as the acrosome state and DNA integrity have shown significant impact on ART outcome. Although fertilization can be achieved with a single spermatozoon of high quality, current quality assessments are population-based and do not allow investigation of multiple sperm characteristics on a single spermatozoon simultaneously. In order to study sperm cells on the single cell level, we designed and characterized a PDMS microfluidic platform that allows single sperm entrapment. After spatially confining individual sperm cells within microfluidic cell traps, the cell viability, chromosomal content and acrosome state were studied. This platform is suitable for the analysis of individual sperm cells, which could be exploited for (non-invasive) sperm analysis and selection by impedance or Raman spectroscopy.

1. Introduction

Nowadays, assisted reproduction technologies (ART) are commonly used to achieve pregnancy. Examples of ART procedures are intrauterine insemination (IUI), *in vitro* fertilization (IVF) and intracytoplasmic sperm injection (ICSI).[1] In order to ensure the highest probability of fertilization, sperm selection techniques such as sperm washing, sperm swim-up and density gradient centrifugation are used to obtain the most motile and viable sperm before performing ART procedures.[2] However, these selection techniques do not target all intrinsic sperm characteristics which have impact on ART outcome.[3,4] Advanced selection techniques focus on additional sperm characteristics such as DNA integrity, apoptosis, membrane maturation and ultramorphology.[3,5]

Ideally, ART procedures are performed using viable, morphologically normal spermatozoa with high DNA integrity and intact plasma and acrosomal membranes. Especially, ICSI treatments are dependent on accurate selection, since only one spermatozoon is used during each procedure. However, most selection procedures and sperm quality-related studies rely on population-based approaches, which are not applicable (yet) on the single cell level. The lack of comprehensive single cell information could explain why sperm selection based on characteristics, which showed correlation with fertilization potential in population-based studies, fails to achieve clinical relevance in ART procedures. As an example, the significance of DNA integrity on reproductive outcome is both supported[6,7] and contradicted.[8,9]

A potential way to manipulate and study spermatozoa on the single cell level is the use of microfluidic technology. In the past decade, a growing number of reports showed the potential to perform sperm handling and selection in microfluidic systems.[10] These systems have shown important advantages over traditional selection techniques such the potential to work with small sample volumes, short processing times and the ability to manipulate single cells. Various reports show the ability to separate spermatozoa by their ability to swim through microchannels,[11,12] to cross laminar flows[13,14] or to swim against fluid flows.[15–17] These microfluidic systems are able to select for viable and motile sperm cells, avoiding induced cell damage inflicted by routine ART procedures. However, these platforms do not allow sperm manipulation and analysis on the single cell level.

Few reports focus on the microfluidic manipulation and analysis of single spermatozoa. In a report by Fuhr *et al.*[18] individual spermatozoa were entrapped using dielectrophoresis, allowing the investigation of the sperm motility. Ohta *et al.*[19] used laser tweezers to entrap spermatozoa based on membrane

[a] *BIOS Lab on a Chip Group, MESA+ and MIRA Institutes, University of Twente, P.O. Box 217, 7500 AE Enschede, The Netherlands. E-mail: b.dewagenaar@utwente.nl*
[b] *Department of Obstetrics and Gynaecology, Radboud University Nijmegen Medical Centre, Nijmegen, The Netherlands*

† Electronic supplementary information (ESI) available. See DOI: 10.1039/c4lc01425a

integrity. In both approaches, complicated methods were used to spatially confine spermatozoa, which are potentially invasive, which limit their use for clinical applications. Furthermore, no extensive analysis of the sperm quality was reported. In previous work of our group, we trapped single spermatozoa on fibronectin spots, allowing automatic analysis of the sperm's motility for ICSI purposes.[20] However, this platform is not suitable for fluorescence staining procedures.

We report the design of a simple PDMS microfluidic platform in which sperm cells were entrapped non-invasively by hydrodynamics. Sperm characteristics such as the cell viability, acrosome state and chromosomal content were studied on individual entrapped sperm cells. This platform allows (non-invasive) analysis on the single cell level and has the potential to be a versatile tool for selection applications or fundamental studies on spermatozoa.

2. Materials and methods

2.1. Microfluidic setup and chip fabrication

The microfluidic chip consists of two main channels, which are interconnected by small side channels (Fig. 1). The chip was designed using CleWin software (version 4.0.1). Master molds for PDMS fabrication were produced by standard photolithography. In short, two layers of SU-8 (Microchem, Berlin, Germany) were spun and developed on 4″ silicon wafers. The first and second layers contain the design features of the side channels and main channels, respectively. Three different SU-8 molds were fabricated, varying the first layer thickness between 1, 1.5 and 2 μm (fabrication results 0.96, 1.49 and 2.2 μm, respectively, Bruker Dektak 8). The total thickness of both layers combined was 20 μm.

Chips were fabricated using PDMS (Sylgard 184, Dow Corning, Midland, MI, USA) in a 1 : 10 v/v ratio of base *versus* curing agent. PDMS was poured onto a silicon wafer, degassed and cured at 60 °C overnight. After curing, microfluidic inlets and outlets were punched using Harris UniCore punchers (tip ID 1.0 and 3.0 mm, Ted Pella Inc., Redding, CA, USA). The chips were bonded to glass microscope slides using oxygen plasma (Harrick PDC-001, NY, USA). Finally, the chips were baked at 60 °C for at least 30 min before use.

2.2. PLL-g-PEG surface coating

PDMS and glass surfaces were coated with poly(L-lysine)-grafted-poly(ethylene glycol) (PLL-g-PEG, SuSoS, Dübendorf, Switzerland) to prevent cell adhesion during cell trapping experiments. PLL-g-PEG was rinsed through the PDMS microchannels at a concentration of 100 μg ml^{-1} in DI water for at least 15 min.

2.3. Sample preparation

Fresh boar semen was obtained from a local artificial insemination centre ("KI Twenthe", Fleringen, The Netherlands) at a concentration of 20 × 10^6 cells ml^{-1}. The samples were diluted with Beltsville Thawning Solution (BTS, Solusem, Aim Worldwide, Vught, The Netherlands) to a concentration of 2 × 10^6 cells ml^{-1} before trapping experiments.

2.4. Hydrodynamic cell trapping

Two 100 μl syringes (Hamilton gastight, 1710N, Reno, NV, USA) were connected to the 1 mm chip outlets using fused silica capillaries (Polymicro Technologies, ID 100 μm, OD 360 μm, Molex, Surrey, UK) and Tygon tubing (ND 100-80, ID 250 μm, OD 760 μm, Saint-Gobain Performance Plastics, Akron, OH, USA). Two constant fluid flows were established by drawing liquid from the 3 mm inlet reservoirs to the outlets using a syringe pump (neMESYS, Cetoni GmbH, Korbussen, Germany). First, channels were rinsed with a PLL-g-PEG coating solution for 15 min at flow rates of 0.25 μl min^{-1} (±208.3 μm s^{-1}). Subsequently, BTS was flushed through the system for 15 min at equal flow rates to remove the remaining coating solution. After introducing the sperm sample to the top channel, the flow rates of the top and bottom channels were adjusted to 0.025 and 2.5 μl min^{-1}, respectively. Due to the resulting pressure difference, cells were

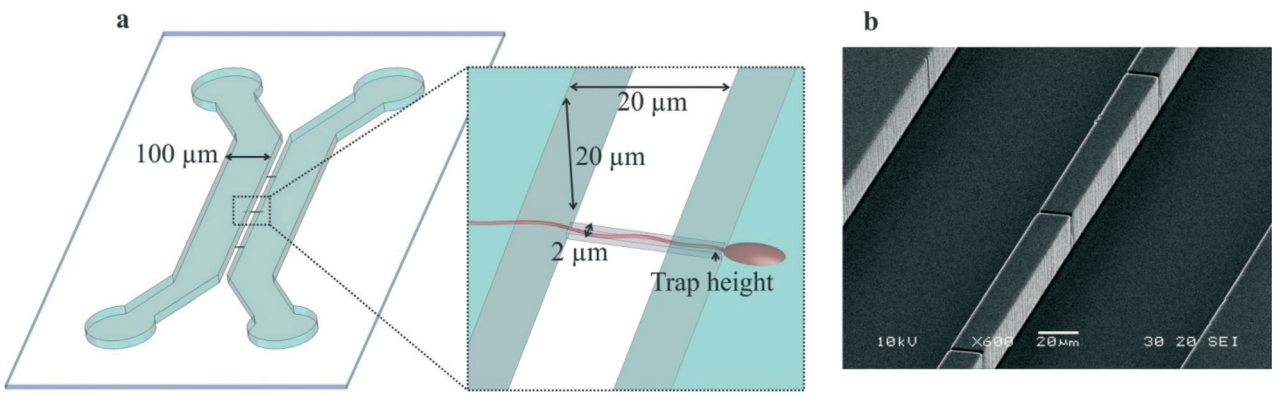

Fig. 1 Illustration and imaging of the microfluidic platform. The PDMS chip design, when bonded to a glass substrate (a), consists of two main channels (width 100 μm, height 20 μm) and twenty side channels (width 2 μm, length 20 μm), which connect the main channels. The height of these side channels, *i.e.* trap height, is 1, 1.5 or 2 μm. The topography of the PDMS device (1 μm high side channels facing upwards) was studied using SEM (b).

trapped within the side channels. Sperm trapping experiments were performed within 1 to 2 minutes. After trapping, the sperm solution was replaced by BTS and a mild pressure difference was retained using top and bottom channel flow rates of 0.025 and 0.5 μl min^{-1} to prevent sperm from escaping from the traps.

2.5. Viability staining

Sperm viability staining was performed (on-chip) using SYTO 9 (ex/em 485/498, Invitrogen, Eugene, OR, USA) and propidium iodide (PI, ex/em 535/617, Life Technologies, Eugene, OR, USA) nucleic stains. Sperm was pre-stained using a BTS solution with 3.34 μM SYTO 9 for 5 min before trapping in the microfluidic device. After trapping, a 10 μg mL^{-1} PI in BTS solution was rinsed through the channel at a flow rate of 0.025 μl min^{-1} at room temperature. Viability of entrapped sperm and non-trapped, control sperm (pipetted on glass slides) was investigated at 15 and 45 min after cell trapping. Each control experiment was performed right after a cell trapping experiment using the same sperm solution. Fresh sperm solutions were prepared before each viability experiment. A Nikon TE2000-U microscope equipped with a 10× phase contrast objective, DS-RI1 camera, Nikon Intensilight C-HGFIE and FITC and PI filter cubes (49011 and 41005, Chroma Technologies, Bellow Falls, VT, USA) was used.

2.6. Fluorescence *in situ* hybridization

The X and Y-chromosomes of sperm cells were stained with fluorescence *in situ* hybridization (FISH) using porcine X- and Y-chromosome specific probes in hybridization buffer (Idetect, IDPF1078 ex/em 493/521 and IDPR1066 ex/em 548/573, ID Labs, London, Canada). The off- and on-chip staining procedures are described separately.

2.6.1. Off-chip staining. FISH staining of sperm cells was based on detailed protocols described elsewhere.[21,22] In short, sperm at a concentration of 1×10^6 cells ml^{-1} was incubated in a 0.075 M KCl (Sigma Aldrich) hypotonic solution at 37 °C for 30 min and fixated using Carnoy's fixative (3 : 1 v/v methanol : acetic acid; Sigma Aldrich) afterwards. After washing the fixated cells with 2× saline-sodium citrate (SSC; Fisher Bioreagents), the cells were incubated in a freshly prepared dithiothreitol (DTT) solution (5 mM 1,4-dithiothreitol, 1% v/v Triton X-100 and 50 mM 2-amino-2-(hydroxymethyl)-1,3-propanediol in DI water; purchased from Acros Organics, Sigma Aldrich and Acros Organics, respectively) at 37 °C for 15 min to decondense the chromatin. After incubation, the cells were washed twice in 2× SSC for 3 min and in ethanol (70%, 85% and 100%) for 1 min each. Subsequently, a hybridization mixture of X and Y-chromosome specific DNA probes and hybridization buffer (50% v/v) was added and co-denatured with the chromosomal DNA at 73 °C for 3 min. Hybridization was performed in polycarbonate hybridization chambers (Corning Inc., NY, USA) at 37 °C overnight. After incubation, the cells were washed using a 0.4× SSC with 0.3% v/v Tween-20 (Acros Organics) washing solution at 73 °C for 3 min. Finally, cells were washed with DI water and mounted with Vectashield (Vector Laboratories, Inc., Burlingame, CA, USA). Fluorescence visualization was performed using an EVOS FL cell imaging system (Life Technologies, Eugene, OR, USA) equipped with a 40× objective and GFP and RFP filter cubes.

2.6.2. On-chip staining. On-chip FISH staining was performed by adapting the previously described FISH protocol. All reagents were rinsed through the channels at a flow rate of 0.05 μl min^{-1} unless mentioned otherwise. First, cell trapping was performed as described in section 2.4. After trapping, a 37 °C solution of 0.075 M KCl was rinsed through both channels for 30 min. A microscope hot plate was used to retain the temperature at 37 °C. After hypotonic treatment, Carnoy's fixative was rinsed through the channels for 10 min to fix the sperm cells. Subsequently, the cells were washed with 2× SSC for 2 min after which they were treated with DTT solution at 37 °C for 20 min. Afterwards, 2× SSC and ethanol washes were performed for 2 min each.

After decondensation, the hybridization mix was added to the cell-containing top channel, while adding hybridization buffer to the bottom channel. After sealing the microfluidic inlets with parafilm, the chips were placed on a hot plate at 73 °C for 3 min to denature the probes and DNA. Afterwards, they were placed in an incubator, allowing hybridization under static flow conditions at 37 °C overnight.

After hybridization, the parafilm was removed and 0.4× SSC washing solution was rinsed through the channels at a flow rate of 0.25 μl min^{-1} for 1 min. The flow was stopped and the chip was placed on a hot plate at 73 °C for 2.5 min. Afterwards, the flow was adjusted to 0.1 μl min^{-1} and 2× SSC, DI water and Vectashield were rinsed through the channels for 1 min each. Finally, the chips were completed by removing the tubing and by covering the inlets and outlets with a coverslip. Finished slides were stored at 4 °C before evaluation using the EVOS FL microscope.

2.7. Acrosome staining

Acrosome staining was performed using a fluorescein-conjugated pisum sativum agglutinin (FITC-PSA, ex/em 422/544, Vector Laboratories, Inc., Burlingame, CA, USA) and LysoTracker blue (DND-22, ex/em 373/422, Life Technologies, Eugene, OR, USA) double stain to distinguish between acrosome-damaged and acrosome intact sperm cells, respectively. After trapping, sperm cells were incubated in BTS solution with 25 μg mL^{-1} FITC-PSA and 2.5 μM LysoTracker blue for 1 h at 37 °C under static flow conditions. After incubation, acrosome staining was visualized using an EVOS FL microscope equipped with a 100× oil immersion objective and DAPI, GFP and RFP filter cubes.

2.8. SEM imaging

Scanning electron microscopy (SEM) images were created using a JEOL JSM 5610 after sputtering a thin layer of

chromium on the PDMS chips using an Emitech chromium sputter coater. All images were recorded at an acceleration potential of 10 kV.

3. Results and discussion

3.1. Device design and simulation

An important requirement of the microfluidic device is the ability to entrap sperm cells individually. The PDMS chip design (Fig. 1a) consists of two main channels, which are interconnected by twenty side channels. These side channels will act as cell traps when a pressure gradient is induced between the main channels. A channel width of 2 μm allows fluid flow between the two main channels but will prevent the sperm cells (head length of 9 μm, width of 4.5 μm and a thickness of 0.5 μm (ref. 23)) from crossing to the other main channel. The height of the side channels, *i.e.* trap height, was varied (1, 1.5 or 2 μm) to optimize single cell trapping. The spacing between the side channels is 150 μm.

The topography of a fabricated PDMS chip with a trap height of 1 μm was visualized by SEM (Fig. 1b and S1†). SEM imaging showed smooth PDMS walls and well-defined cell traps.

To study the fluid dynamics in this microfluidic chip, a COMSOL Multiphysics model (version 4.4) was constructed (Fig. 2). This model describes a laminar flow of incompressible fluid (water) through the microfluidic device under no slip conditions, applying zero pressure at the main channel inlets and fluid outflow velocities at the channel outlets. Due to the difference in outflow velocity (0.025 *versus* 2.5 μl min^{-1}), a pressure gradient is formed over the side channels (Fig. 2a). As a result, a flow of fluid is induced within these channels. This fluid flow is illustrated by a fluid velocity field (Fig. 2b) and by flow streamlines (Fig. S2†). In practice, this fluid displacement will drag and entrap passing sperm cells within the side channels.

The pressure difference over a cell trap depends on the distance between the trap and the main channel outlet, *i.e.* cell trap number. The first trap is located closest to the outlet; the last trap is located near the channel inlet. The pressure difference is observed to linearly decrease with increasing distance, *i.e.* increasing trap number (Fig. S3†). According to this simulation, traps close to the channel outlet will likely be the first to entrap sperm in trapping experiments. In the scenario in which trapped sperm cells completely block the fluid flow through the side channels, the fluid flow through the neighbouring, unfilled side channels will gradually increase upon cell trapping. Consequently, the distance between the cell traps and channel outlet will not influence their cell trapping capability. However, a trapped sperm cell will never completely block the fluid flow through a side channel since its thickness is only half the size of the channel height. This leakage flow will affect the trapping capability of neighbouring cell traps. Therefore, we expect to observe a decrease in trap occupancy with increasing distance between trap and channel outlet.

3.2. Single cell entrapment

Sperm trapping was performed using side channels with a height of 1, 1.5 and 2 μm to find the optimal trap height for single sperm entrapment. A typical trapping experiment can be observed in Movie S1.† Cell trapping was performed within 1 to 2 minutes after applying the pressure difference. Experiments showed effective single cell trapping using 1 μm high traps (Fig. 3a). Entrapped sperm cells were orientated in

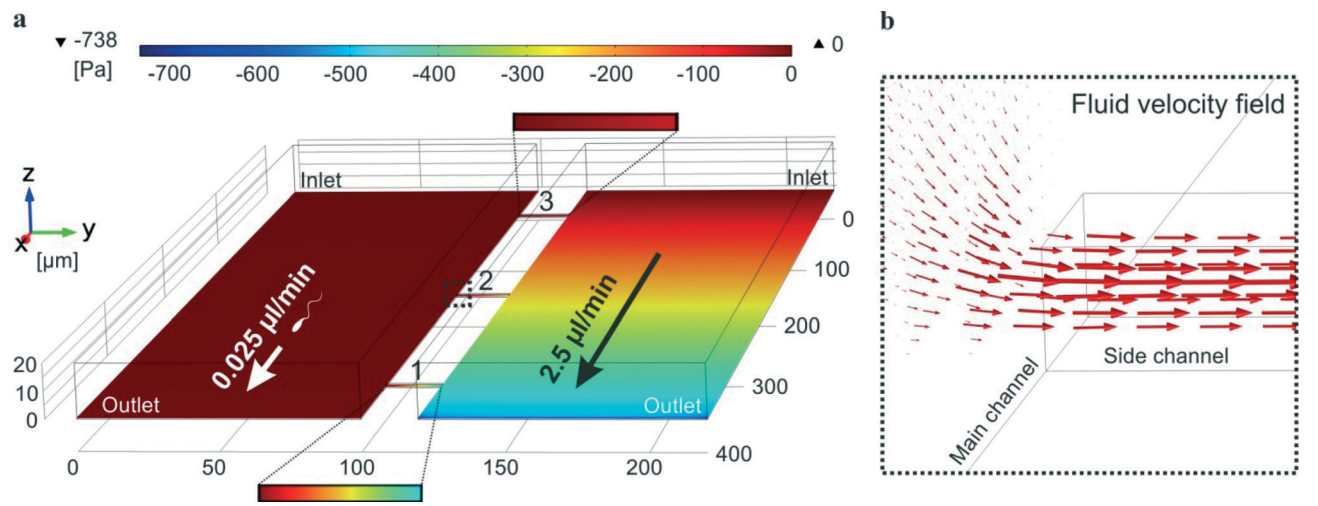

Fig. 2 COMSOL Multiphysics (version 4.4) simulation of the fluid flow within the microfluidic trapping device (a), showing the first three cell traps. A fluid flow of 0.025 μl min^{-1} and 2.5 μl min^{-1} is applied to the left and right main channels, respectively. Due to the difference in flow rates, a pressure gradient is created between the main channels. This is illustrated by the pressure distribution within the device at a height of 0.5 μm, which is half the height of the side channels. As a result of this pressure difference, which is dependent on the distance between the trap and channel outlet (*i.e.* trap number), a fluid flow is induced through these side channels. This fluid flow is illustrated by arrows representing the direction and magnitude of the fluid flow (b).

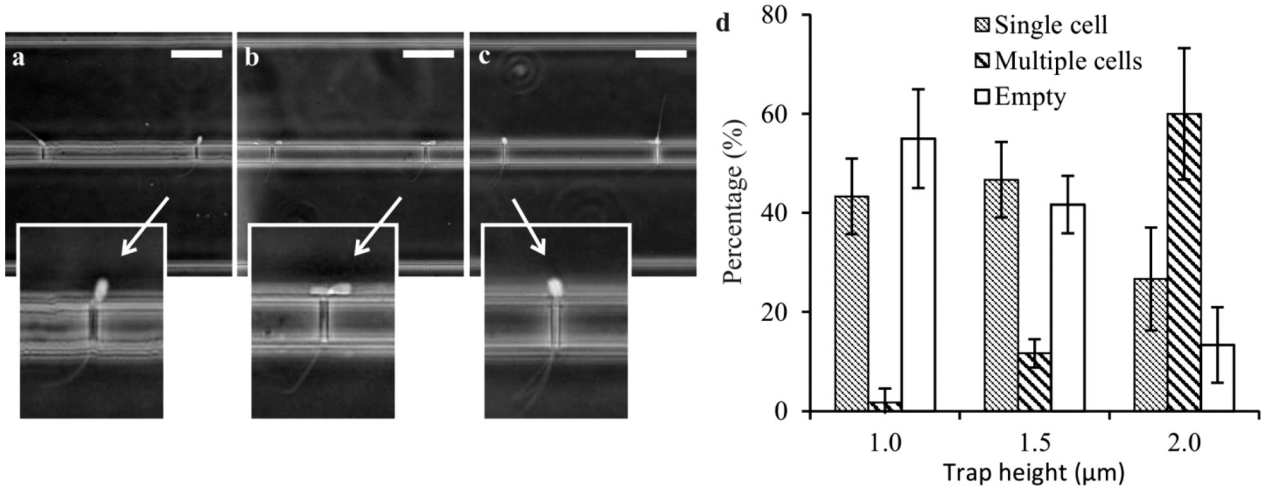

Fig. 3 Entrapment of sperm cells in 2 μm wide PDMS traps with a height of 1 μm (a), 1.5 μm (b) and 2 μm (c). Sperm cells were entrapped in a head-first or tail-first orientation. The percentage of traps filled with no cells, a single cell or multiple cells was recorded and plotted *versus* trap height (d). The percentage of single cell trapping was highest for chips with a trapping height of 1.5 μm. The highest ratio of single *versus* multiple cell trapping was obtained using chips with a trap height of 1 μm. Increasing the trap height resulted in an increase in multiple cell trapping and a decrease in the amount of empty traps (experiments per trap height n = 3, all scale bars 50 μm).

a head-first or tail-first orientation with respect to the cell trap, in which the tail-first position proved to be the most stable. The 1.5 μm traps showed single sperm entrapment although occasionally two sperm cells were caught in a single trap (Fig. 3b). Increasing the height to 2 μm resulted in an increase in multiple cell trapping (Fig. 3c), catching up to 5 sperm cells per spot. Furthermore, an increased number of sperm cells was caught with their heads in a perpendicular direction with respect to the cell trap, *i.e.* aligning the flat side of their heads with the PDMS wall.

After each trapping experiment, the percentage of empty traps, traps containing a single cell or traps containing multiple cells on each chip, was recorded independently of the trap number. This percentage was clearly influenced by the cell trap height (Fig. 3d, n = 3). The highest ratio of single *versus* multiple cell trapping was obtained using chips with 1 μm high traps. This ratio was observed to decrease with increasing trap height. Unfortunately, the highest amount of empty traps was observed using a trap height of 1 μm. Despite this drawback, a trapping height of 1 μm was considered most suitable for single sperm trapping and analysis.

Now, chips with 1 μm high cell traps were used to investigate the trapping efficiency (Fig. 4). In total, 20 trapping experiments were performed as described in section 2.4. After each experiment, the trap occupancy was recorded for every cell trap in order to calculate the trapping efficiency. This efficiency is expressed as the percentage of successful cell entrapment over all experiments. For example, trap 1 showed 90% efficiency, *i.e.* in 90% of all experiments a sperm cell was entrapped. The data do not show a clear trend; both linear and polynomial trends do not show statistical significance (data not shown). However, the efficiency decreased with trap number, which is in good correspondence with our expectations from the simulation.

3.3. Viability staining

The hydrodynamic trapping procedure could inflict a harmful effect on the sperm. To investigate this effect, the viability was assessed by monitoring the plasma membrane integrity using SYTO 9 and PI nucleic acid stains at two different time points (Fig. 5). Cell membrane permeable SYTO 9 stain (green excitation) is able to bind to the DNA of sperm with intact plasma membranes (*i.e.* viable sperm). However, PI dye (red excitation) is only able to bind to the DNA of sperm with damaged plasma membranes (*i.e.* non-viable sperm). As an example, three entrapped sperm cells showed intact plasma membranes after 15 min (Fig. 5a) and one deteriorated membrane after 45 min (Fig. 5b). The decrease in green intensity after 45 min was caused by photobleaching of the green fluorophore.

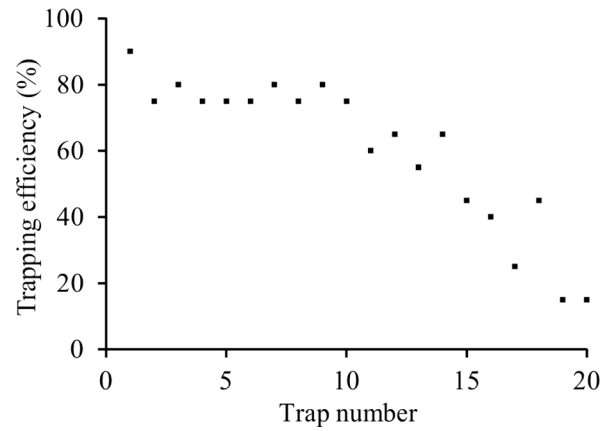

Fig. 4 The cell trapping efficiency as a function of trap number. A clear decrease in efficiency is observed between traps 10 and 20 (n = 20).

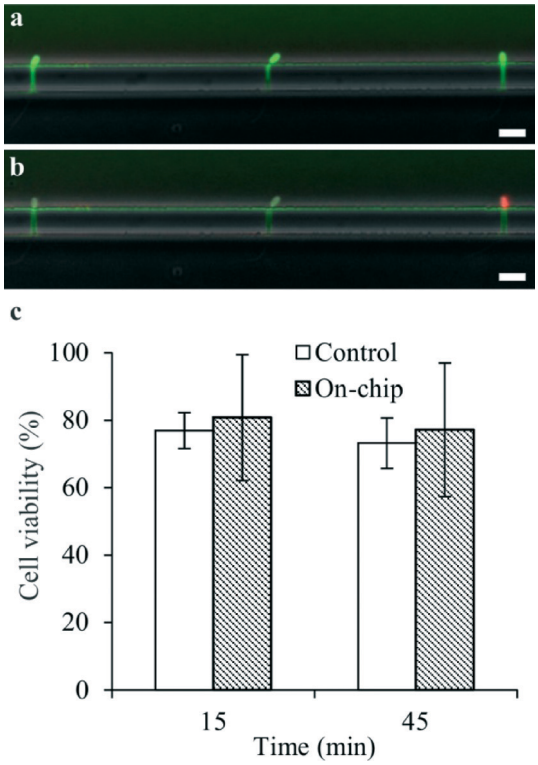

Fig. 5 Cell viability staining of trapped sperm cells using a SYTO 9/PI solution. The viability was monitored at 15 min (a) and 45 min (b) after cell trapping. Photobleaching of the green fluorophore resulted in the loss of green fluorescence intensity after 45 min. Viable sperm cells with intact membranes were visualized by a clear green fluorescence signal; deterioration of the plasma membrane was indicated by a red fluorescence signal. No difference in viability was observed between the control and on-chip group (c). Furthermore, no decrease in cell viability was observed for both control and entrapped sperm cells after 45 min (n = 7, all scale bars 20 μm).

The cell viability was assessed by separate viability experiments. Cell counts were 122 ± 30 (average ± s.d.) for each control experiment and 15 ± 2 for each on-chip experiment (n = 7). High cell viability was observed for both the control and the on-chip group (Fig. 5c). The sperm viability of both groups remained constant over time. No significant differences in viability were observed between both groups at both time points, indicating that the viability of the entrapped sperm was not compromised by the trapping procedure. Furthermore, the non-invasive nature of the trapping procedure was supported by observing motile sperm cells within the microfluidic traps after the trapping procedure (Movie S2†).

All viability experiments were performed using PDMS devices in which the surface coating was performed using optimized procedures. Coating with old PLL-g-PEG solution (>1 week) or a prolonged duration between chip bonding and coating (>30 min) showed a negative effect on cell viability (data not shown). No clear explanation was found for this observation. Potentially, a reduced surface coverage played a role in the decrease in sperm viability. The literature on PLL-g-PEG coating of PDMS shows that the absorption of polymer on oxidized surfaces is higher compared to absorption on hydrophobic surfaces.[24,25] Bad surface coverage could result in direct contact between the PDMS surface and sperm cells upon cell trapping. Although PDMS is biocompatible in general, the fragile nature of sperm could be compromised by leaching of absorbed trace elements[26] or hydrophobic materials such as PDMS uncrosslinked oligomers.[27] In short, a decreased PLL-g-PEG surface coverage due to its reduced absorption on hydrophobic PDMS surfaces could result in the increase of leaching of toxic components, resulting in a decrease of sperm viability.

3.4. FISH

FISH is a commonly used technique to investigate chromosome content and chromosomal anomalies of sperm, such as sperm aneuploidy.[28] The presence of chromosomal anomalies has shown correlation with male infertility[29] and ICSI outcome.[30] To test whether chromosome analysis can be performed on entrapped sperm cells in the current microfluidic device, a FISH procedure was designed on-chip. In this example, the sex chromosome content was investigated using X and Y-chromosome specific DNA probes.

FISH control experiments showed successful hybridization of the two DNA probes on the X and Y-chromosomes, indicated by green and red fluorescence signals, respectively

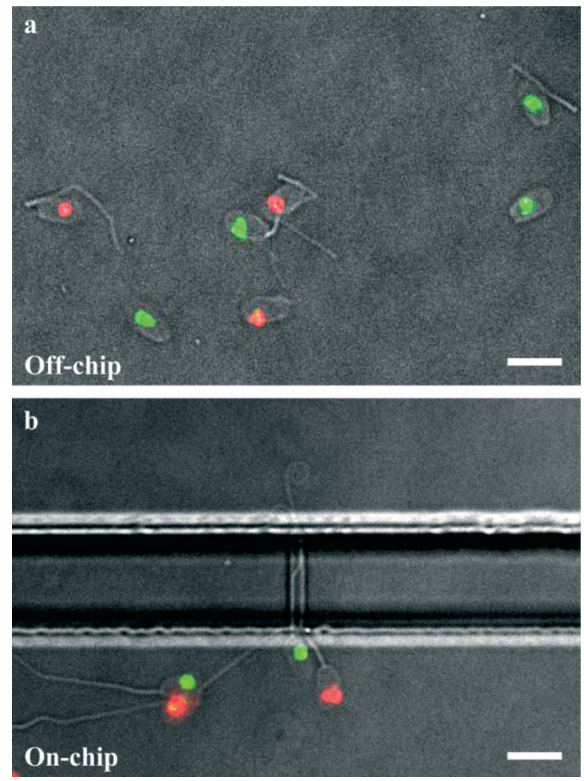

Fig. 6 Fluorescence *in situ* hybridization of the X and Y-chromosomes, yielding sperm cells with a green or red fluorescence signal, respectively (a). This staining protocol was performed on-chip (b) to investigate the sex-chromosome content of entrapped sperm cells (all scale bars 10 μm).

(Fig. 6a). The staining technique was performed on-chip, yielding entrapped sperm cells with stained X- and Y-chromosomes (Fig. 6b). In this experiment, chips were used with a trap height of 2 μm without PLL-g-PEG surface coating, which explains the number of multiple entrapped sperm cells. These results show the potential to perform FISH analysis on-chip, allowing the analysis of chromosomal anomalies of individually trapped sperm.

3.5. Acrosome staining

The acrosome reaction, which involves the activation of proteolytic enzymes to digest the zona pellucida, plays a crucial role in the fertilizing potential of spermatozoa.[31] *In vitro* analysis using the ionophore-induced acrosome reaction (ARIC) test was shown to be effective in predicting fertilization potential in IUI and IVF treatments.[32]

Analysis of the acrosome state of entrapped sperm cells was performed using FITC-PSA and LysoTracker blue, staining acrosome-reacted and acrosome-intact sperm, respectively. This double acrosome staining was combined with PI, allowing investigation of the integrity of the acrosomal and plasma membranes simultaneously. Bonding of PSA to exposed lectins of damaged acrosomal membranes resulted in a clear green fluorescence (Fig. 7a–c). Non-specific green fluorescence was caused by particles of non-dissolved PSA, which were trapped aside from the sperm cells. Sperm cells with intact acrosomes were identified by the absence of lectin-bound PSA and the presence of LysoTracker blue. Absorption of the LysoTracker dye in the weak acidic environment (pH ≈ 5) of an intact acrosome yielded a clear blue fluorescence signal (Fig. 7a). Despite the high background fluorescence due to absorbed fluorophore within the PDMS matrix, sperm cells with intact acrosomes could be distinguished on-chip (Fig. 7d, inset). Potentially, this absorption can be reduced or prevented by coating the chips with a layer of parylene.[33] Furthermore, the use of different fabrication materials such as glass or thermoplastics such as polymethylmethacrylate and cyclo-olefin copolymer could prevent dye absorption. However, the use of these materials could increase the complexity and costs of device fabrication.

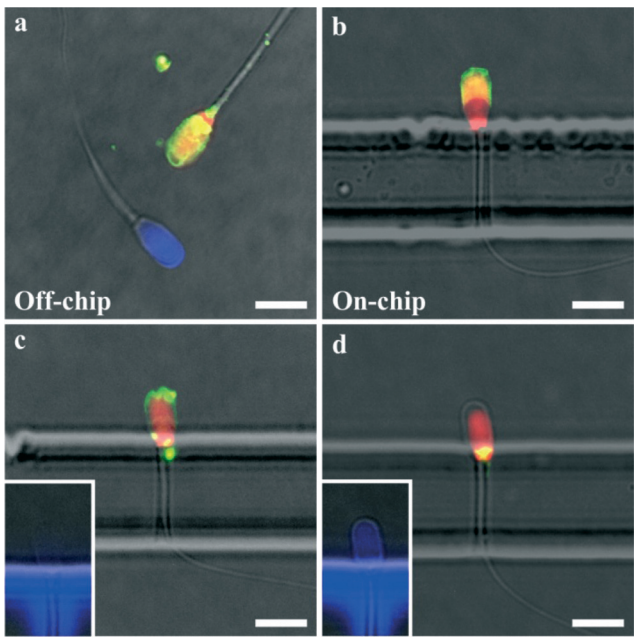

Fig. 7 Acrosome staining of sperm cells. Reacted and unreacted acrosomes were visualized using FITC-PSA and LysoTracker blue, respectively (a). PI was used to test the integrity of the plasma membrane. This staining procedure was used to evaluate the acrosome state of sperm cells trapped on-chip. Sperm cells with damaged or reacted acrosomes showed specific FITC-PSA staining (b and c) and the absence of LysoTracker stain (inset of c). Intact acrosomes were observed by the absence of FITC-PSA staining (d) and the absorption of LysoTracker stain (inset of d) (all scale bars 10 μm).

3.6. Device implementation

The potential of the presented microfluidic device to spatially confine individual sperm cells allows the analysis of sperm on the single cell level. However, the current analysis techniques depend on the use of fluorescent labels, which limits the use of entrapped sperm cells after analysis. Therefore, single cell analysis must be performed label-free and non-invasively to retain good sperm quality for ART applications after analysis. Two promising techniques are Raman and impedance spectroscopy. Raman spectroscopy has been successfully applied on the micro-scale to study single cell properties in microfluidic (PDMS) platforms.[34] This technique was used to study DNA damage and the acrosomal membrane of sperm cells,[35,36] although no studies have been conducted on viable spermatozoa so far due to practical challenges. On the contrary, numerous reports show the use of impedance spectroscopy to study viable cells non-invasively using microfluidic (PDMS) platforms.[37–39] Therefore, our future work will focus on the characterization of the sperm quality using impedance spectroscopy. The fluorescence staining procedures described in this report will be used for verification purposes.

Besides integrating the trapping device with a non-invasive analysis technique, this platform must allow the recovery of single spermatozoa selectively for ART applications. Selective cell recovery can be accomplished by multiplexing the current design with recovery channels. These can be designed in close proximity to the cell traps allowing single cell recovery using hydrodynamics. Alternatively, small diameter needles may be used to pick up single sperm cells as shown in previous work.[20]

4. Conclusions

In this study, we designed and characterized a microfluidic platform for the entrapment and analysis of single sperm cells. Effective single cell entrapment was accomplished using a hydrodynamic trapping procedure using rectangular cell traps with a width of 2 μm and a height of 1 μm. Single cell analysis was performed on entrapped sperm cells,

studying the sperm viability, chromosome content and acrosome state. In future, this platform can be exploited for the advanced analysis of individual sperm cells. Furthermore, this platform can be integrated with non-invasive analysis methods, such as Raman and impedance spectroscopy, to utilize non-invasive analysis and selection for ART purposes.

Acknowledgements

Financial support from the NWO – Netherlands Organization of Scientific Research (Spinoza grants to A. van den Berg and Veni L.I. Segerink), the scientific support of N. Huisintveld, J.P. Frimat, C.C.L. Denoeud, I. van de Ven, C. Velraeds and S. Sukas and the technical support of P.M. ter Braak is gratefully acknowledged. We also thank the "KI Twenthe" for the kind supply of boar semen samples.

Notes and references

1 A. P. Ferraretti, V. Goossens, J. de Mouzon, S. Bhattacharya, J. A. Castilla, V. Korsak, M. Kupka, K. G. Nygren and A. Nyboe Andersen, T. E. IVF-monitoring, f. t. E. S. o. H. R. Consortium and Embryology, *Hum. Reprod.*, 2012, **27**, 2571–2584.
2 R. R. Henkel and W. B. Schill, *Reprod. Biol. Endocrinol.*, 2003, **1**, 108.
3 T. M. Said and J. A. Land, *Hum. Reprod. Update*, 2011, **17**, 719–733.
4 I. Yetunde and M. Vasiliki, *Minerva Ginecol.*, 2013, **65**, 487–496.
5 R. Henkel, *Asian J. Androl.*, 2012, **14**, 260–269.
6 M. Benchaib, V. Braun, J. Lornage, S. Hadj, B. Salle, H. Lejeune and J. F. Guerin, *Hum. Reprod.*, 2003, **18**, 1023–1028.
7 K. L. Larson, C. J. DeJonge, A. M. Barnes, L. K. Jost and D. P. Evenson, *Hum. Reprod.*, 2000, **15**, 1717–1722.
8 S. Pfeifer, *Fertil. Steril.*, 2014, **101**, 884–884.
9 A. S. R. Med, *Fertil. Steril.*, 2008, **90**, S178–S180.
10 J. E. Swain, D. Lai, S. Takayama and G. D. Smith, *Lab Chip*, 2013, **13**, 1213–1224.
11 S. Tasoglu, H. Safaee, X. H. Zhang, J. L. Kingsley, P. N. Catalano, U. A. Gurkan, A. Nureddin, E. Kayaalp, R. M. Anchan, R. L. Maas, E. Tuzel and U. Demirci, *Small*, 2013, **9**, 3374–3384.
12 R. Nosrati, M. Vollmer, L. Eamer, M. C. San Gabriel, K. Zeidan, A. Zini and D. Sinton, *Lab Chip*, 2014, **14**, 1142–1150.
13 B. S. Cho, T. G. Schuster, X. Zhu, D. Chang, G. D. Smith and S. Takayama, *Anal. Chem.*, 2003, **75**, 1671–1675.
14 K. Matsuura, M. Takenami, Y. Kuroda, T. Hyakutake, S. Yanase and K. Naruse, *Reprod. BioMed. Online*, 2012, **24**, 109–115.
15 D. B. Seo, Y. Agca, Z. C. Feng and J. K. Critser, *Microfluid. Nanofluid.*, 2007, **3**, 561–570.
16 T. Qiu, C. Han, R. Ma, L. Xie, Z. Li, K. Su, L. Wang, G. Huang, J. Wang, J. Qiao, W. Xing and J. Cheng, *Solid-State Sensors, Actuators and Microsystems Conference (TRANSDUCERS), 2011 16th International*, 2011, pp. 1320–1323.
17 M. D. Lopez-Garcia, R. L. Monson, K. Haubert, M. B. Wheeler and D. J. Beebe, *Biomed. Microdevices*, 2008, **10**, 709–718.
18 G. Fuhr, T. Müller, V. Baukloh and K. Lucas, *Hum. Reprod.*, 1998, **13**, 136–141.
19 A. T. Ohta, M. Garcia, J. K. Valley, L. Banie, H. Y. Hsu, A. Jamshidi, S. L. Neale, T. Lue and M. C. Wu, *Lab Chip*, 2010, **10**, 3213–3217.
20 J. P. Frimat, M. Bronkhorst, B. de Wagenaar, J. G. Bomer, F. van der Heijden, A. van den Berg and L. I. Segerink, *Lab Chip*, 2014, **14**, 2635–2641.
21 I. Parrilla, J. M. Vazquez, M. Oliver-Bonet, J. Navarro, J. Yelamos, J. Roca and E. A. Martinez, *Reproduction*, 2003, **126**, 317–325.
22 Z. Sarrate and E. Anton, *J. Visualized Exp.*, 2009, 31.
23 F. Saravia, I. Núñez-Martínez, J. M. Morán, C. Soler, A. Muriel, H. Rodríguez-Martínez and F. J. Peña, *Theriogenology*, 2007, **68**, 196–203.
24 S. Lee and J. Voros, *Langmuir*, 2005, **21**, 11957–11962.
25 S. Lee and N. D. Spencer, *Langmuir*, 2008, **24**, 9479–9488.
26 U. Marzec-Wroblewska, P. Kaminski and P. Lakota, *Folia Biol.*, 2012, **58**, 7–15.
27 K. J. Regehr, M. Domenech, J. T. Koepsel, K. C. Carver, S. J. Ellison-Zelski, W. L. Murphy, L. A. Schuler, E. T. Alarid and D. J. Beebe, *Lab Chip*, 2009, **9**, 2132–2139.
28 A. E. Calogero, N. Burrello, A. De Palma, N. Barone, R. D'Agata and E. Vicari, *Reprod. BioMed. Online*, 2003, **6**, 310–317.
29 S. Egozcue, J. Blanco, J. M. Vendrell, F. Garcia, A. Veiga, B. Aran, P. N. Barri, F. Vidal and J. Egozcue, *Hum. Reprod. Update*, 2000, **6**, 93–105.
30 C. Rubio, M. Gil-Salom, C. Simon, L. Rodrigo, Y. Minguez, J. Remohi and A. Pellicer, *Hum. Reprod.*, 2001, **16**, 2084–2092.
31 S. C. Esteves and S. Verza Jr., *Open Reprod. Sci. J.*, 2011, **3**, 13.
32 T. Katsuki, T. Hara, K. Ueda, J. Tanaka and K. Ohama, *Hum. Reprod.*, 2005, **20**, 469–475.
33 H. Sasaki, H. Onoe, T. Osaki, R. Kawano and S. Takeuchi, *Sens. Actuators, B*, 2010, **150**, 478–482.
34 R. D. Snook, T. J. Harvey, E. C. Faria and P. Gardner, *Integr. Biol.*, 2009, **1**, 43–52.
35 N. Li, D. Chen, Y. Xu, S. Liu and H. Zhang, *Biomed. Opt. Express*, 2014, **5**, 1690–1699.
36 C. Mallidis, J. Wistuba, B. Bleisteiner, O. S. Damm, P. Gross, F. Wubbeling, C. Fallnich, M. Burger and S. Schlatt, *Hum. Reprod.*, 2011, **26**, 1641–1649.
37 D. Malleo, J. T. Nevill, L. P. Lee and H. Morgan, *Microfluid. Nanofluid.*, 2010, **9**, 191–198.
38 T. Sun and H. Morgan, *Microfluid. Nanofluid.*, 2010, **8**, 423–443.
39 D. Mondal, C. Roychaudhuri, L. Das and J. Chatterjee, *Biomed. Microdevices*, 2012, **14**, 955–964.